Supporting Information

Rational design of an HClO-specific triggered self-immolative fluorescent turn-on sensor and its bioimaging applications

Xiao-Bo Wang[a,b], Da-Long Zhang[c], Hui-Jing Li[a,*], Xuhao Lu[a], Quanze Liu[a], and Yan-Chao Wu[a,b*]

[a] *Weihai Marine Organism & Medical Technology Research Institute, Harbin Institute of Technology, Weihai 264209, China*

[b] *Henan Key Laboratory of Biomolecular Recognition and Sensing (Shangqiu Normal University).*

[c] *Tianjin Disha Pharmaceutical Technology Development Co., Ltd, Tianjin 300071, China*

Table S1 Comparison of Fluorescent Sensors for HClO Detection

Sensors	Time needed to reach FI plateau	Detection media	LOD	Applications	ref
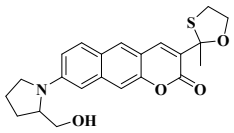	within seconds	PBS containing 1% DMSO	34.8	Cell imaging, Tissue imaging	1
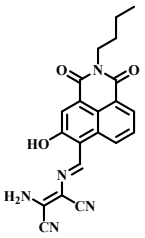	4 s	DMSO:PBS = 3:7	17.3 nM	Cell imaging, Zebrafish imaging, Mouse arthritis imaging	2
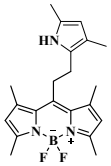	1 s	EtOH:PBS = 1:9	0.56 nM	Cell imaging	3
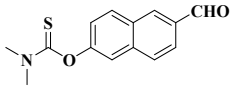	25 s	PBS	2.37 nM	Cell imaging	4
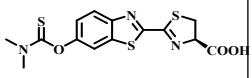	1 h	Tris-HCl buffer (10 mM $MgCl_2$)	33 nM	Cell imaging, Mouse imaging	5
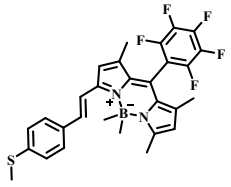	——	DMF:PBS = 1:1	59 nM	Cell imaging, Zebra fish imging, Liver Disease Mouse Model imaging	6
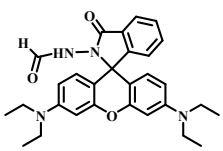	3 s	PBS	0.116 nM	Cell imaging, Zebra fish imging	7
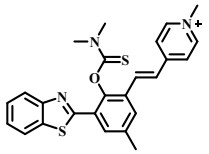	65 s	HEPES:MeOH = 4:1	0.47 μM	Cell imaging, C. elegans imaging, Mouse imaging	8
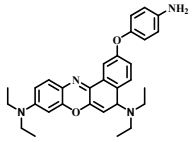	1 min	PBS:DMSO = 95:5	4.37 μM	Cell imaging, Tissue imaging, Mouse imaging	9

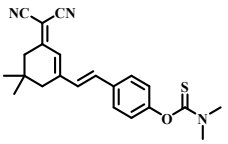	3 s	100% aqueous solution	88.06 nM	Cell imaging	10
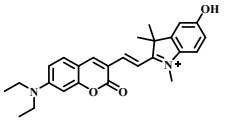	2 min	PBS	49.1 nM	Cell imaging, Zebrafish imaging, Mouse arthritis imaging	11
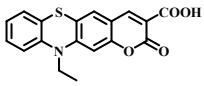	100 s	PBS	16.1 nM	Cell imaging, Mouse arthritis imaging	12
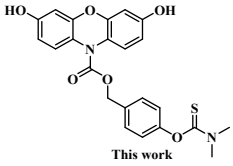	10 s	PBS	16.8 nM	Test strips, Cell imaging, Zebrafish imaging, Mouse arthritis imaging	This work

Main Instruments and Reagents

All reagents in this work were purchased from commercial sources. Column chromatography silica gel used in the experiment was 200–300 mesh. The NMR spectra were recorded on the AVANCE II spectrometer with tetramethylsilane (TMS) as the reference. High resolution mass spectrometry analysis (HRMS) was carried out by Bruker APEX IV spectrometer. T6 new century spectrometer was used for UV-Visible spectrum measurements. All the Fluorescence spectra measurements were carried out on the FluoroMax-4 fluorescence spectrophotometer. Fluorescence imaging of cells and zebra fish were carried out on OLYMPUS FV1200 MPE confocal imaging system. Fluorescence imaging of mouse were performed on a PerkinElmer IVIS Spectrum imaging system.

Procedure for spectral measurements

The sensor **RESClO** was dissolved in dimethyl sulfoxide (DMSO) to prepare a 1 mM stock solution. During the test, an appropriate volume of stock solution was diluted to 10 μM with 10 mM PBS solution (pH = 7.4), and then shaken well enough for testing. HClO was diluted to 1 mM

in deionized water using NaClO solution with 14.5% effective chlorine content, and then diluted to the appropriate concentration for testing as required. Other ROS/RNS were then diluted to the appropriate concentration in the buffer solution as required for the test. If not stated, the excitation wavelength was 560 nm, and the emission wavelength was collected at 565–700 nm for all fluorescence tests.

Preparation of reactive oxygen species (ROS) and reactive nitrogen species (RNS)

HClO The concentration of HOCl was determined by using its molar extinction coefficient of 391 $M^{-1}cm^{-1}$ at 292 nm before use.

O_2^- Superoxide was generated from KO_2. KO_2 and 18-crown-6 ether (2.5 eq) was dissolved in DMSO to afford a 0.25 M solution.

•HO Hydroxyl radical was generated by the Fenton reaction. To prepare •OH solution, hydrogen peroxide (H_2O_2, 10 eq) was added to $Fe(ClO_4)_2$ in deionised water.

NO Nitric oxide was generated from potassium nitroprusside dihydrate.

$^1O_2$ Singlet oxygen was generated from the Na_2MoO_4-H_2O_2 system in 0.05 M carbonate buffer of pH 10.5

$ONOO^-$ Simultaneously, 0.6 M KNO_2, 0.6 M in HC1, 0.7 M in H_2O_2 was added at to a 3 M NaOH solution at 0 ºC. The concentration of peroxynitrite was estimated by using extinction coefficient of 1670 cm^{-1} M^{-1} at 302 nm in 0.1 M sodium hydroxide aqueous solutions.

The synthesis of Compound 1, 2, RE-NH and RE-BTC

Synthesis of compound **2**: To a solution of 4-Hydroxybenzaldehyde (0.30 g, 2.46 mmol) in DCM (5 mL) was added N,N-Dimethylaminothioformyl chloride (0.30 g, 2.46 mmol) at room

temperature. Then two drops Et_3N was added into the reaction solution. The reaction mixture was stirred for 3 h at room temperature. The organic solvent was removed in vacuum to afford the compound 1 for use in the next step. To a solution of compound 1 (0.20 g, 0.96 mmol) was added $NaBH_4$ (40 mg, 1.0 mmol) at 0 ˚C. The reaction mixture was stirred for 0.5 h. The mixture was poured into ice water and extracted with DCM. The organic layer was dried with Na_2SO_4 and concentrated to get compound 2 without further purification. ^{1}H NMR (400 MHz, $CDCl_3$): δ 7.49 (d, *J* = 8.4 Hz, 2H), 7.06 (d, *J* = 8.4 Hz, 2H), 4.68 (s, 2H), 3.46 (s, 3H), 3.36 (s, 3H); ^{13}C NMR (100 MHz, $CDCl_3$): δ 187.8, 153.4, 138.7, 127.8, 122.8, 64.7, 43.3, 38.8.

Synthesis of compound **RE-NH**: A solution of Zn powder (1.30 g, 19.91 mmol), resazurin sodium salt (1.00 g, 3.98 mmol), and glacial acetic acid (20 mL) were stirred vigorously at ambient temperature for 2 h under an atmosphere of N_2. After the reaction mixture was rapidlyremoved under vacuum and the residues were dissolved in acetone (20 mL). *N, N*-dimethyl-4- aminopyridine (0.49 g, 3.98 mmol) was added to the reaction solution in a portion. Then acetic anhydride (0.76 mL, 7.96 mmol) was added dropwisely to the reaction solution. The mixture was stirred for 3 h. Removal of Zn powder by Celite flitration, the filtrate mixture was evaporated under vacuum to get a yellow crude product. Compound **RE-NH** was isolated as a white solid by silica-gel column chromatography in 71% yield (850 mg). ^{1}H NMR (400 MHz, Acetone-d_6): δ 7.35 (s, 1H), 6.47–6.54 (m, 6H), 2.20 (s, 6H); ^{13}C NMR (100 MHz, Acetone-d_6): δ 169.8, 145.7, 143.7, 130.9, 117.6, 114.0, 110.6, 20.9; HRMS (ESI): calcd for $C_{16}H_{13}NO_5$ ($[M+Na]^+$): 322.0686, found: 322.0687.

Synthesis of compound **RE-BTC**: Under an N_2 atmosphere, to a solution of compound **RE-NH** (0.50 g, 1.67 mmol), Na_2CO_3 (0.36 g, 3.34 mmol) and *N, N*-dimethyl-4-aminopyridine (0.20 g,

1.67 mmol) in DCM (10 mL) was added dropwise a solution of triphosgene (0.99 g, 3.34 mmol) in DCM (5 mL) at 0 ˚C. The reaction mixture was stirred at ambient temperature under an N_2 atmosphere for 3 h. The reaction mixture was poured into ice water and extracted with DCM. The organic layer was dried with Na_2SO_4, concentrated, and isolated to get compound **RE-BTC** as a white solid by silica-gel column chromatography in 76% yield (460 mg). ^{1}H NMR (400 MHz, $CDCl_3$): δ 7.60 (d, *J* = 8.8 Hz, 2H), 6.97 (d, *J* = 2.6 Hz, 2H), 6.93 (dd, *J* = 2.6, 8.8 Hz, 2H), 2.31 (s, 6H); ^{13}C NMR (100 MHz, $CDCl_3$): δ 168.9, 151.2, 149.7, 148.5, 126.1, 125.6, 117.1, 111.0, 21.1.

Determination of the detection limits

The detection limit was calculated according to the method used in the previous literature.[13–16] The fluorescence intensity at 590 nm was plotted versus the concentrations of HClO. The detection limit was calculated with the following equation:

Detection limit =3 σ / k

Where σ is the standard deviation of blank measurement, k is the slope between the fluorescence intensity versus HClO concentration.

Cytotoxicity assays

The cell viability of RAW 264.7 cells, treated with sensor **RESClO**, was assessed by a cell counting kit-8 (CCK-8; Dojindo Molecular Technologies, Tokyo, Japan). Briefly, RAW 264.7 cells, seeded at a density of 1×10^6 cells·mL^{-1} on a 96-well plate, were maintained at 37 °C in a 5% CO_2/95% air incubator for 12 h. Then the live cells were incubated with various concentrations (0, 5, 10, 20, and 30 μM) of sensor **RESClO** suspended in culture medium for 24 h. Subsequently, CCK-8 solution was added into each well for 2 h, and absorbance at 450 nm was measured.

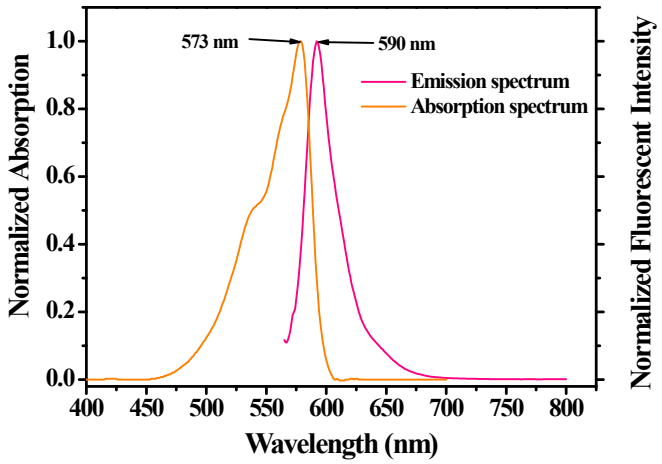

Figure S1 After addition of HClO, the normalized fluorescence emission and absorption spectra of the sensor **RESClO.**

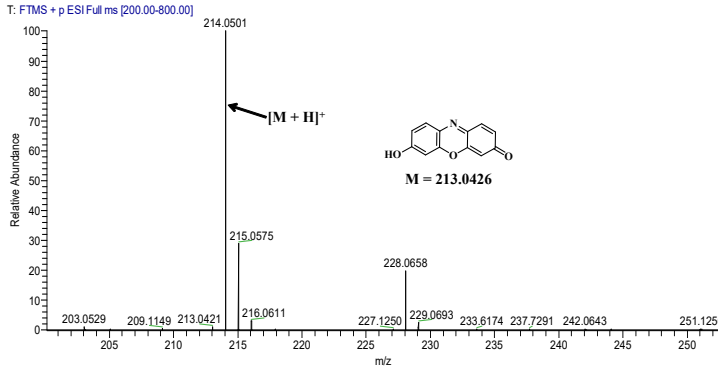

Figure S2 HRMS of reaction product of the sensor **RESClO** and HClO.

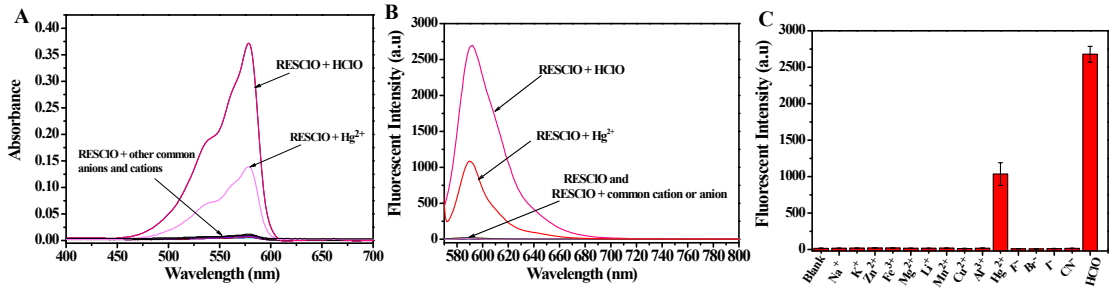

Figure S3 Absorption (A) and fluorescence (B) spectra changes of sensor **RESClO** (10 μM) in PBS buffer solution (10 mM, pH = 7.4) in the presence of HClO (20 μM) and other species (50 μM), including Na^+ , K^+ , Zn^{2+}, Fe^{3+}, Mg^{2+}, Li^+ , Mn^{2+}, Cu^{2+}, Al^{3+} Hg^{2+}, F^-, Br^-, I^-, CN^-; (C) Fluorescence intensity at 590 nm changes after addition of different species for 1 min.

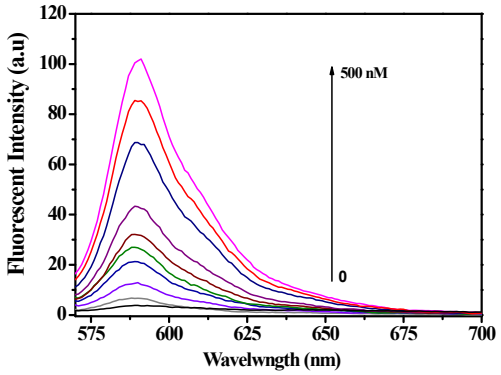

Figure S4 Fluorescence spectra of the sensor **RESClO** (10 μM) in PBS buffer solution (10 mM, pH = 7.4) after addition of different low concentrations of HClO (0, 30, 50, 80, 100, 150, 200, 300, 400, 500 nM).

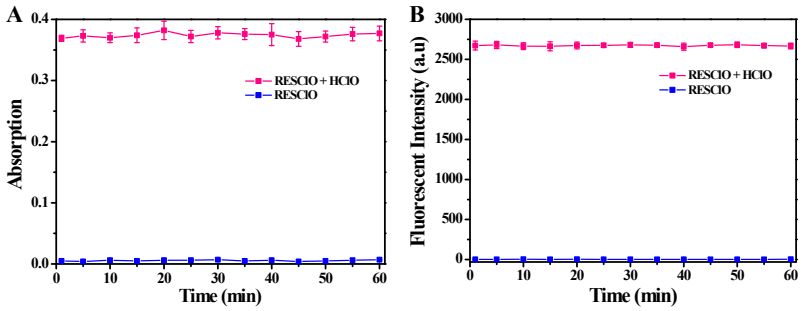

Figure S5 The variation of absorption (A) and fluorescence intensity (B) of the sensor **RESClO** (10 μM) in PBS buffer solution (10 mM, pH = 7.4) with time before and after the addition of HClO (20 μM).

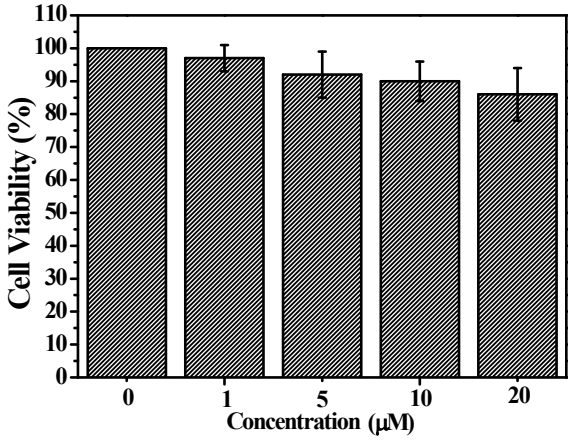

Figure S6 Viability of RAW 264.7 cells treated with various concentrations (0 - 20 μM) of **RESClO** for 24 h. Error bars represent mean values ± SD. (n = 3).

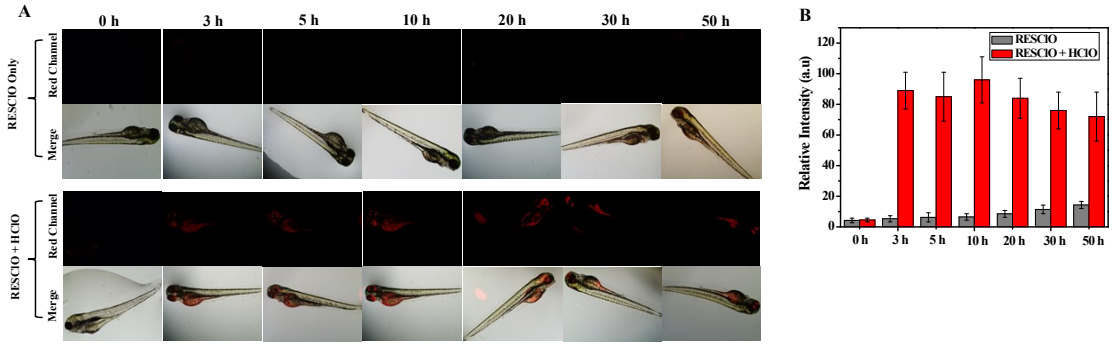

Figure S7 (A) Fluorescent imaging images of zebrafish incubated with the sensor **RESClO** (10 μM) for different times in the presence or absence of HClO (10 μM). (B) Relative fluorescence intensity from corresponding zebra fish.

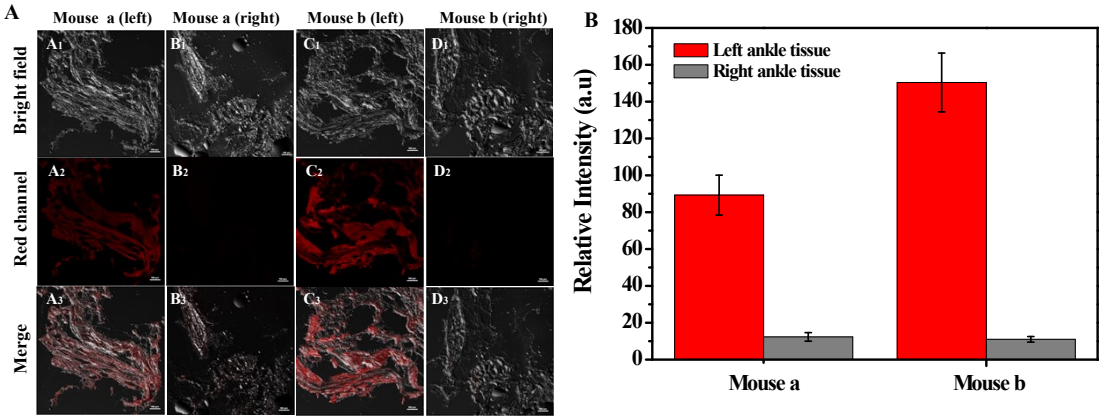

Figure S8 Fluorescence images of frozen slice prepared from mice with different degrees of arthritis induced by 5 mg/mL λ-carrageenan (A_1-A_3: 50 μL; C_1-C_3: 100 μL). Arthritic tissue: Slice isolated from the arthritic area of the left ankle (A_1-A_3 and C_1-C_3). Control: Slice isolated from the right ankle (B_1-B_3 and D_1-D_3). λ_{ex} = 559 nm, λ_{em} = 580−620 nm for the red channel.

Copies of NMR and mass spectra

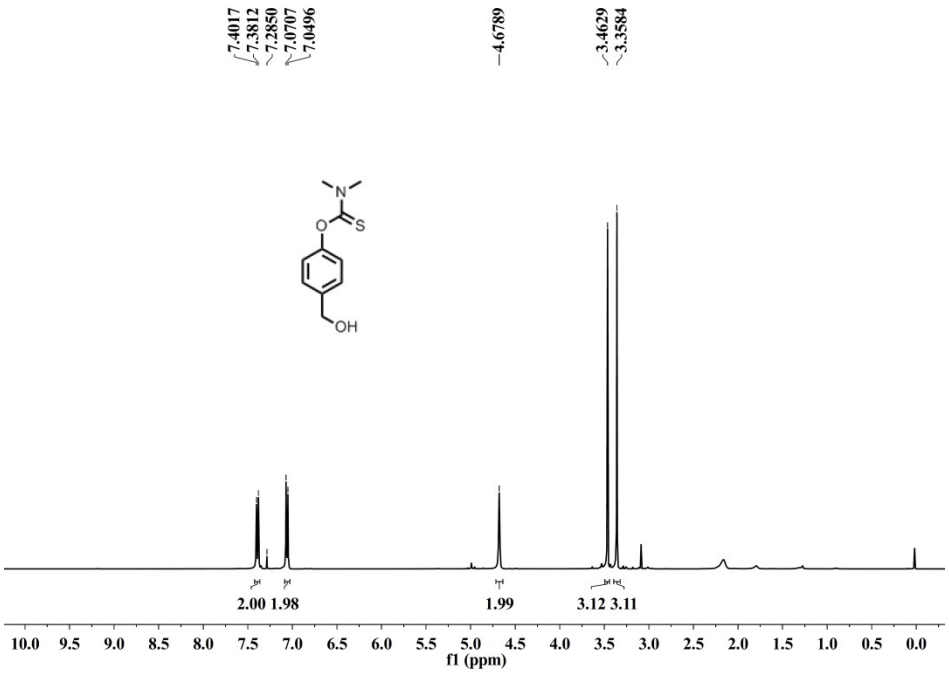

Figire S8 ^{1}H NMR spectrum of compound **2** in $CDCl_3$.

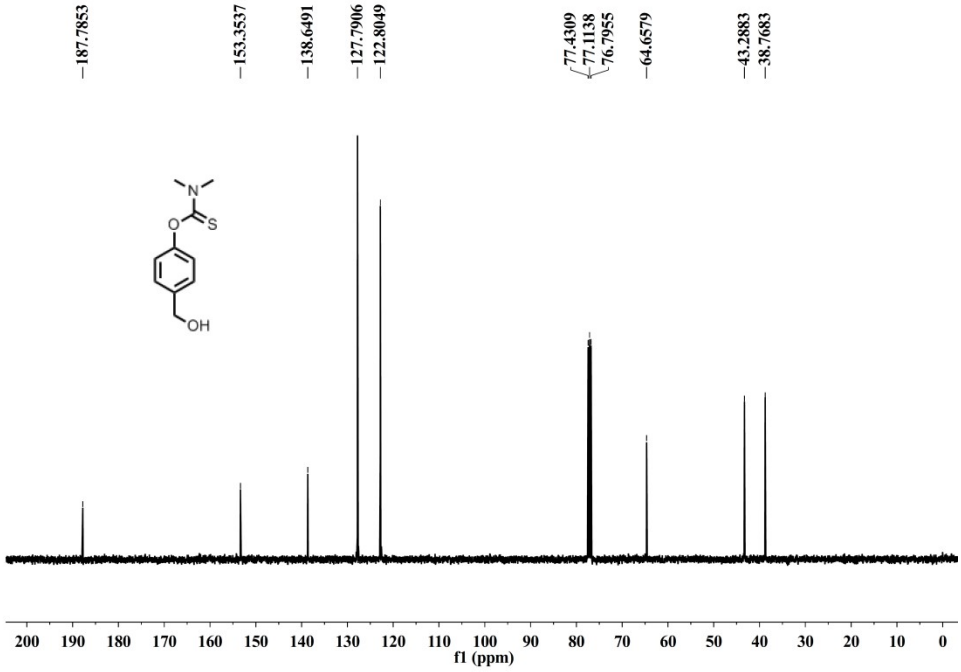

Figure S9 ^{13}C NMR spectrum of compound **2** in $CDCl_3$.

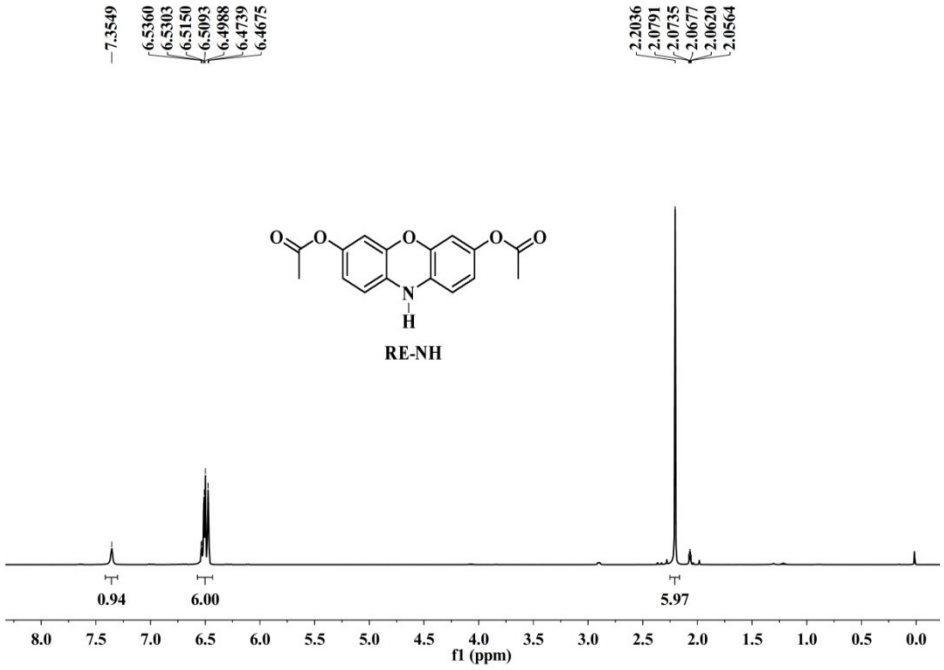

Figure S10 ^{1}H NMR spectrum of compound **RE-NH** in Acetone-$d_{6.}$

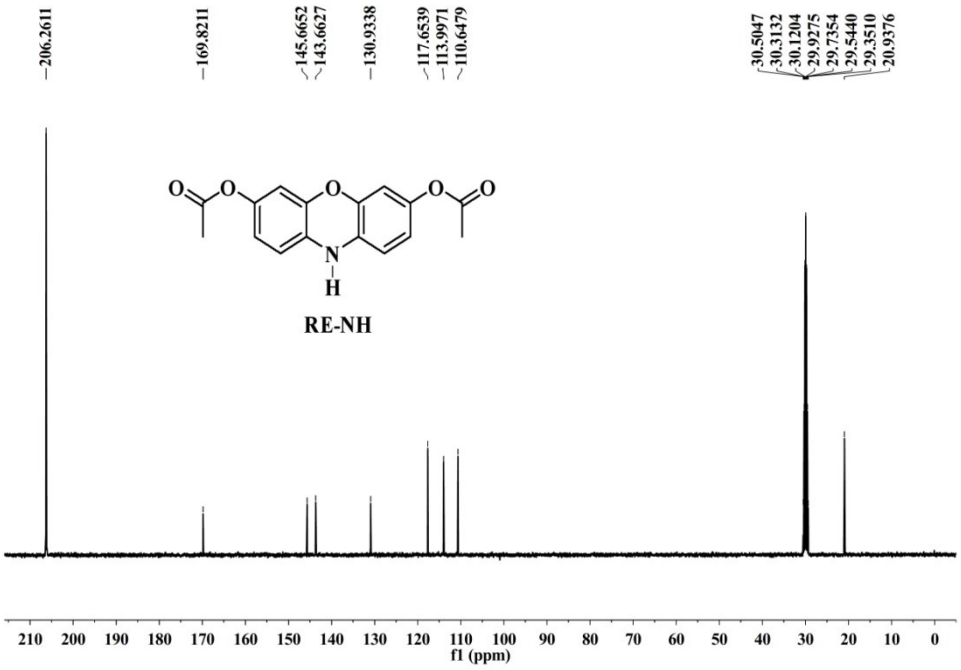

Figure S11 ^{13}C NMR spectrum of compound **RE-NH** in Acetone- $-d_{6.}$

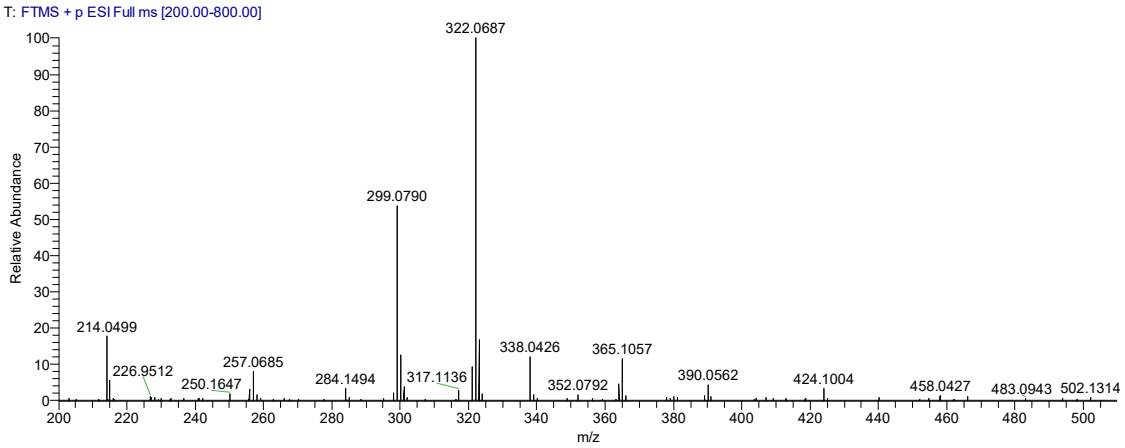

Figure S12 HRMS spectrum of compound **RE-NH**

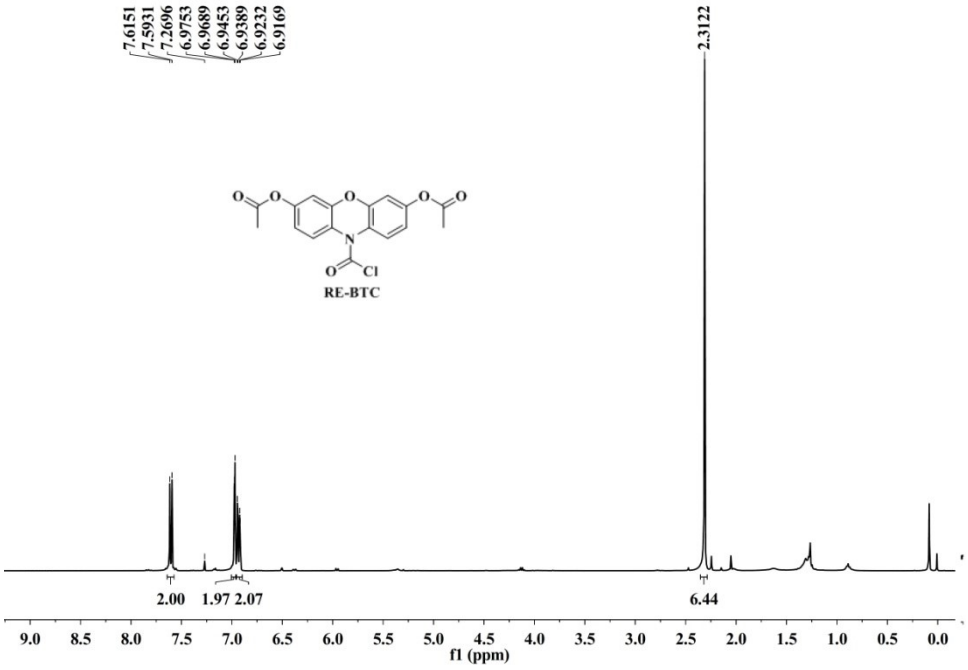

Figure S13 ^{1}H NMR spectrum of compound **RE-BTC** in $CDCl_3$.

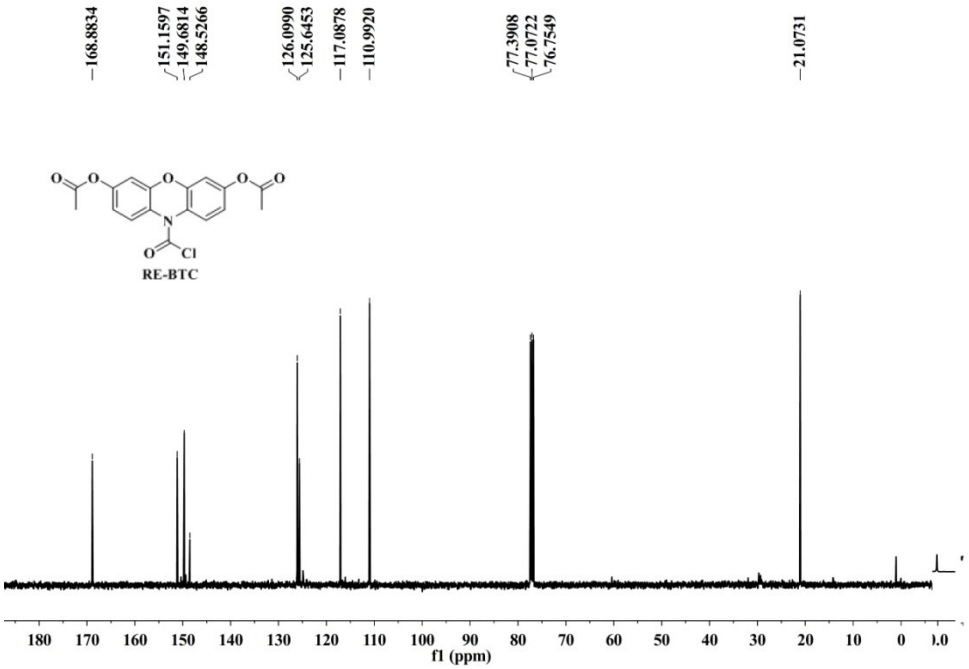

Figure S14 ^{13}C NMR spectrum of compound **RE-BTC** in $CDCl_3$.

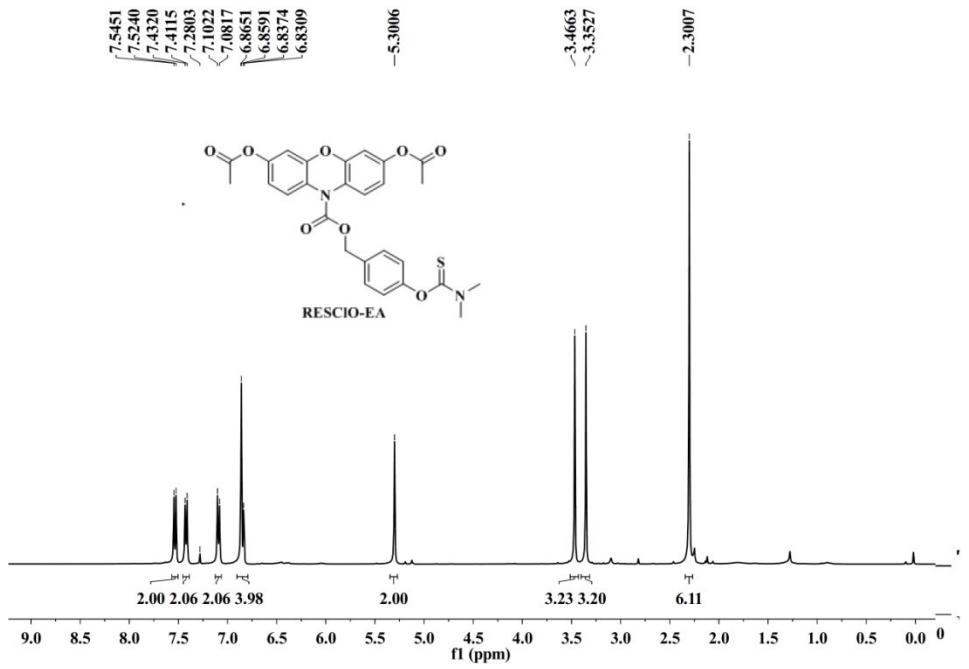

Figure S15 ^{1}H NMR spectrum of compound **RESClO-EA** in $CDCl_3$.

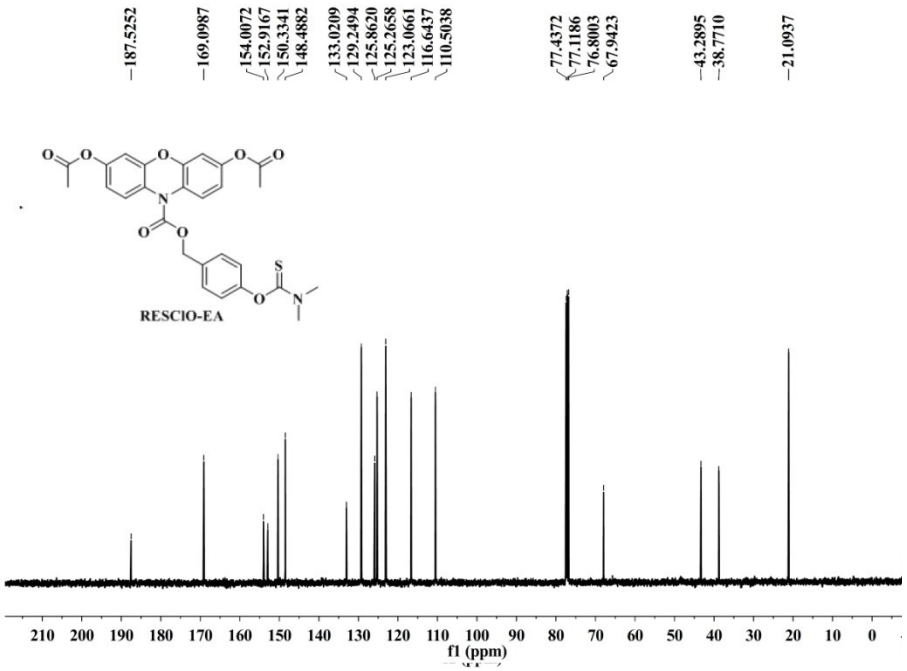

Figure S16 ^{13}C NMR spectrum of compound **RESClO-EA** in $CDCl_3$.

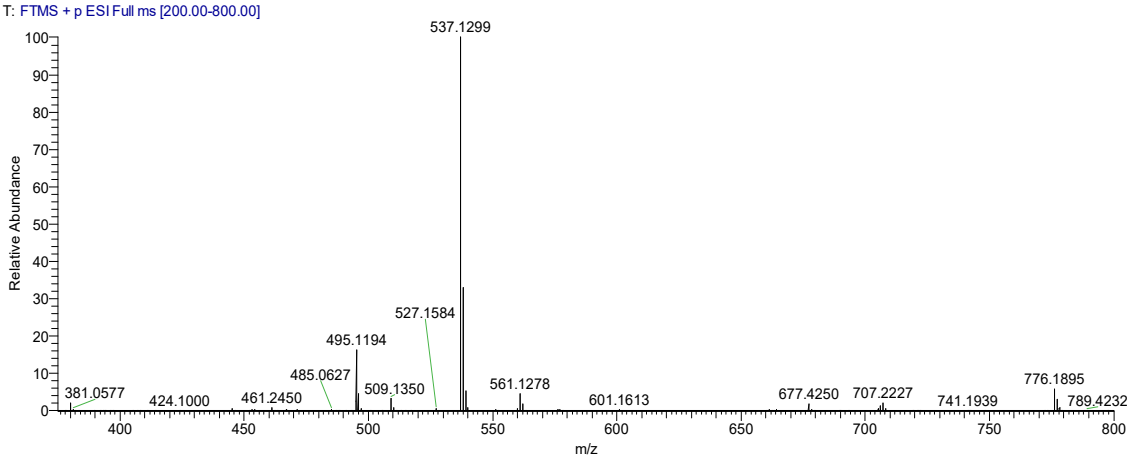

Figure S17 HRMS spectrum of **RESClO-EA**.

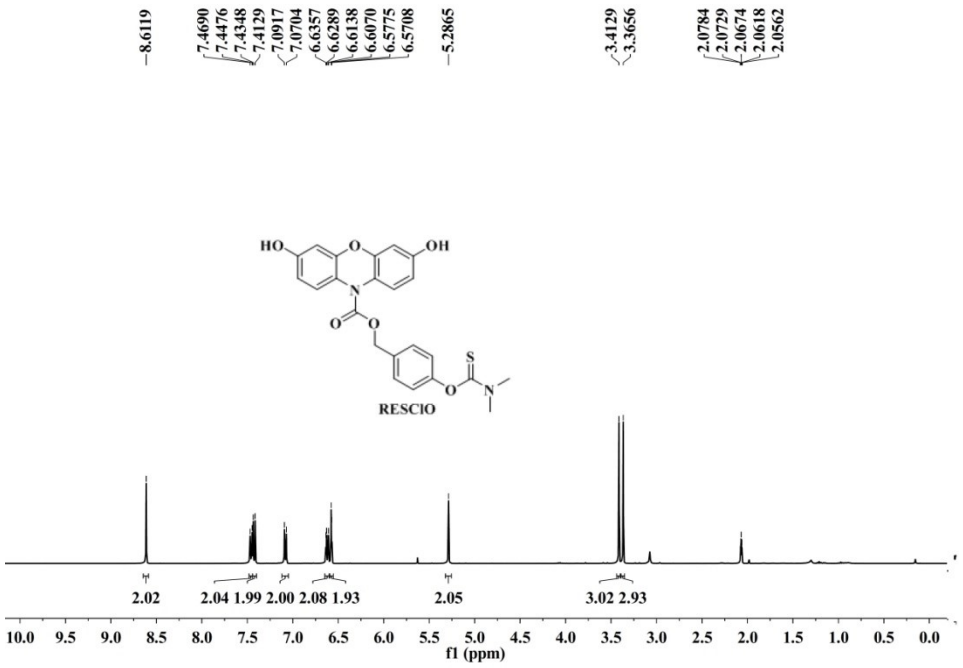

Figure S18 [1]H NMR spectrum of compound **RESClO** in Acetone-d_6.

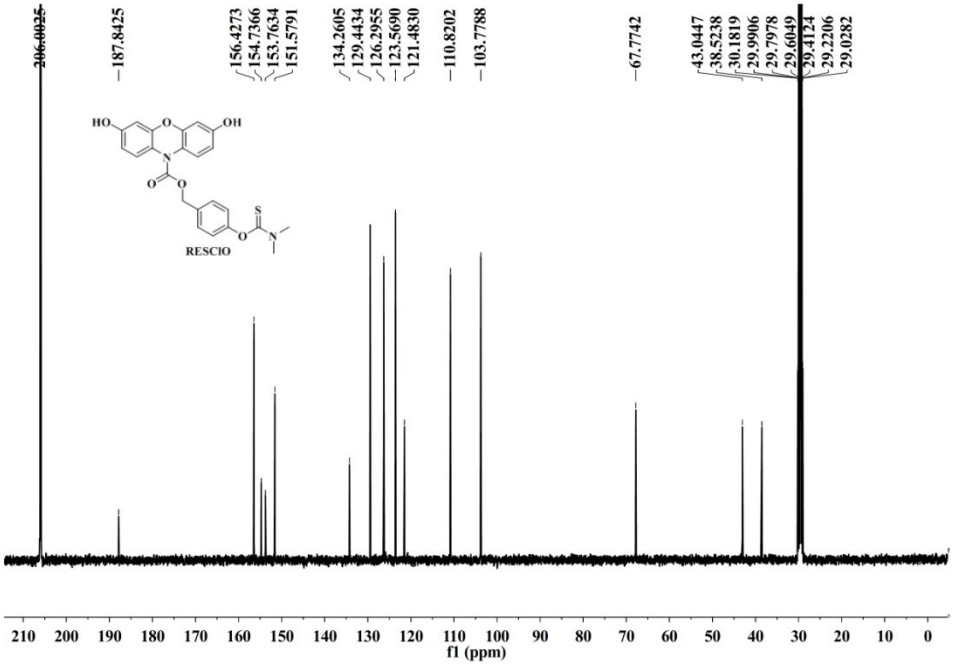

Figure S19 [13]C NMR spectrum of compound **RESClO** in Acetone-d_6.

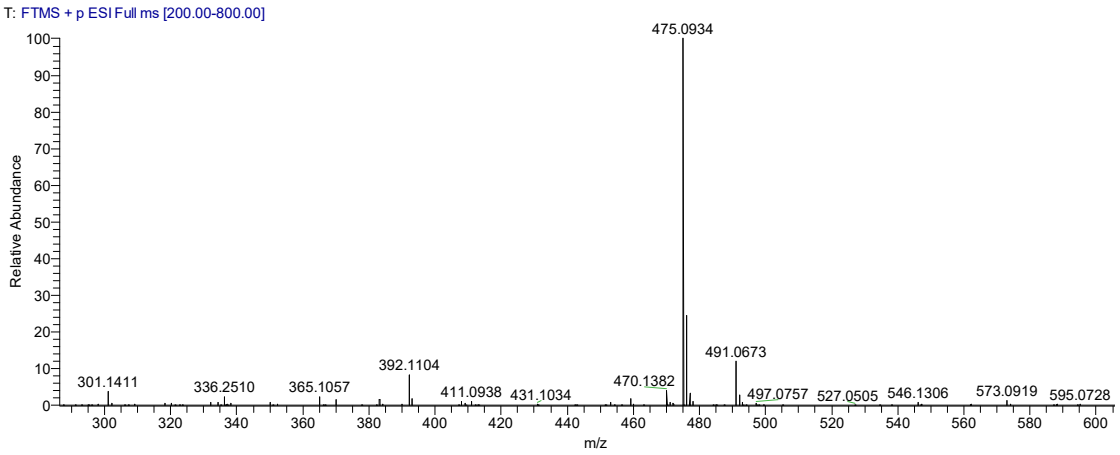

Figure S20 HRMS spectrum of **RESClO**.

References

[1] Y. W. Jun, S. Sarkar, S. Singha, Y. J. Reo, H. R. Kim, J.-J Kim, K. H Ahn, A two-photon fluorescent probe for ratiometric imaging of endogenous hypochlorous acid in live cells and tissues. Chem. Comm., 53(2017), 10800–10803.

[2] H. Feng, Z. Zhang, Q. Meng, H. Jia, Y. Wang, R. Zhang, Rapid Response Fluorescence Probe Enabled In Vivo Diagnosis and Assessing Treatment Response of Hypochlorous Acid-Mediated Rheumatoid Arthritis, Adv. Sci. 5 (2018) 1800397.

[3] H. Zhu, J. Fan, J. Wang, H. Mu, X. Peng, An "enhanced PET"-based fluorescent probe with ultrasensitivity for imaging basal and elesclomol-induced HClO in cancer cells. J. Am. Chem. Soc.136 (2014), 12820–12823.

[4] Y. Jiang, G. Zheng, Q. Duan, L. Yang, J. Zhang, H. Zhang, D. Ho, Ultra-sensitive fluorescent probes for hypochlorite acid detection and exogenous/endogenous imaging of living cells. Chem. Comm. 54 (2018), 7967–7970.

[5] C. Tang, Y. Gao, T. Liu, Y. Lin, X. Zhang, C. Zhang, X. Li, T. Zhang, L. Du, M. Li, Bioluminescent Probe for Detecting Endogenous Hypochlorite in Living Mice, Org. Bio. Chem. 16 (2018) 645–651.

[6] C. Duan, M. Won, P. Verwilst, J. Xu, H.S. Kim, L. Zeng, J.S. Kim, In Vivo Imaging of Endogenously Produced HClO in Zebrafish and Mice Using a Bright, Photostable Ratiometric Fluorescent Probe, Anal. Chem. 91 (2019) 4172–4178.

[7] C. Liu, Z. Li, C. Yu, Y. Chen, D. Liu, Zhuang, P. Jia, H. Zhu, X. Zhang, Y. Yu, Development of a Concise Rhodamine-Formylhydrazine Type Fluorescent Probe for Highly Specific and Ultrasensitive Tracing of Basal HOCl in Live Cells and Zebrafish, ACS Sensors 4 (2019) 2156–

2163.

[8] D. Shi, S. Chen, B. Dong, Y. Zhang, C. Sheng, T.D. James, Y. Guo, Evaluation of HOCl-Generating Anticancer Agents by an Ultrasensitive Dual-Mode Fluorescent Probe, Chem. Sci. 10 (2019) 3715–3722.

[9] X. Lin, Y. Chen, L. Bao, S. Wang, K. Liu, W. Qin, F. Kong, A Two-Photon near-Infrared Fluorescent Probe for Imaging Endogenous Hypochlorite in Cells, Tissue and Living Mouse，Dyes Pigments 174 (2020) 108113.

[10] Y. Zhang, Y. Ma, Z. Wang, X. Zhang, X. Chen, S. Hou, H. Wang, A Novel Colorimetric and Far-Red Emission Ratiometric Fluorescent Probe for the Highly Selective and Ultrafast Detection of Hypochlorite in Water and Its Application in Bioimaging, Analyst 145 (2020) 939–945.

[11] J.S. Lan,, L. Liu, R.F. Zeng, Y.H. Qin, Y. Liu, X.Y. Jiang, A. Aihemaiti, Y. Ding, T. Zhang, R.J. Y. Ho, Rational Modulation of Coumarin-Hemicyanine Platform Based on OH Substitution for Higher Selective Detection of Hypochlorite, Chem. Comm. 56 (2020) 1219–1222.

[12] J.T. Hou, B. Wang, Y. Zou, P. Fan, X. Chang, X. Cao, S. Wang, F. Yu, Molecular Fluorescent Probes for Imaging and Evaluation of Hypochlorite Fluctuations during Diagnosis and Therapy of Osteoarthritis in Cells and in a Mouse Model, ACS Sensors 5 (2020) 1949–1958.

[13] W. Chen, H. Luo, X. Liu, J. W. Foley, X. Song, Broadly Applicable Strategy for the Fluorescence Based Detection and Differentiation of Glutathione and Cysteine/Homocysteine: Demonstration in Vitro and in Vivo, Anal. Chem. 88 (2016), 3638-3646.

[14] Y. C. Liao, P. Venkatesan, L. F. Wei, S. P. Wu, A coumarin-based fluorescent probe for thiols and its application in cell imaging, Sens. Actuators B: Chem. 232 (2016), 732-737.

[15] T. Liu, F. Huo, C. Yin, J. Li, J. Chao, Y. Zhang, A triphenylamine as a fluorophore and

maleimide as a bonding group selective turn-on fluorescent imaging probe for thiols, Dyes Pigments 128 (2016), 209-214.

[16] W. Lin, L. Long, W. Tan, A Highly Sensitive Fluorescent Probe for Detection of Benzenethiols in Environmental Samples and Living Cells, Chem. Comm. 46 (2010) 1503–1505.